

# Structure and mechanical properties of bulk glass-forming Ni–Nb–Sn alloys

Haein Choi-Yim <sup>a,\*</sup>, Donghua Xu <sup>d</sup>, Mary Laura Lind <sup>b</sup>,  
Jörg F. Löffler <sup>c</sup>, William L. Johnson <sup>b</sup>

<sup>a</sup> Department of Physics, Sookmyung Women's University, Seoul 140-742, Republic of Korea

<sup>b</sup> W.M. Keck Laboratory of Engineering Materials, Mail Code 138-78, California Institute of Technology, Pasadena, CA 91125, USA

<sup>c</sup> Laboratory of Metal Physics and Technology, Department of Materials, Wolfgang-Pauli-Str. 10, ETH Zürich, CH-8093 Zürich, Switzerland

<sup>d</sup> Department of Nuclear Engineering, University of California, Berkeley, CA 94720-1730, USA

Received 2 August 2005; received in revised form 21 September 2005; accepted 22 September 2005

Available online 20 October 2005

## Abstract

Ternary alloys of composition  $\text{Ni}_{60}\text{Nb}_{40-x}\text{Sn}_x$ , with  $3 \leq x < 9$ , were found to form bulk metallic glasses. These alloys exhibit a high elastic modulus and measured compressive yield strength between 1.8 and 2.8 GPa. The measured yield strength of these ternary alloys depends strongly on their Sn content and is generally lower than the strength estimated from modulus and hardness. The tendency to phase separation suggested by small-angle neutron scattering experiments is used to account for the obvious discrepancy between the measured and the theoretical strengths.

© 2005 Acta Materialia Inc. Published by Elsevier Ltd. All rights reserved.

**Keywords:** Metallic glasses; Composites; Mechanical properties; Phase separation

## 1. Introduction

In the past few decades many bulk metallic glass-forming systems with high glass-forming ability (GFA) and good stability with respect to crystallization have been developed [1–3]. Among the bulk metallic glasses (BMGs) discovered, zirconium-based alloys (of the “Vitroloy”-type Zr–Ti–Ni–Cu–Be) are exceptionally processable [3]. These BMGs possess various desirable properties which include their high yield strength, hardness, and elastic strain limit in addition to reasonably high fracture toughness, fatigue resistance, and corrosion resistance. Zr-based glasses have found many applications, having already been cast into items such as sporting goods, surgical instruments, and strong, thin cases for electronic devices such as cellphones.

The unique properties of BMGs provide a strong impetus for identifying new processable metallic glass-forming alloys with even greater strength, elastic moduli, hardness, and ductility. Especially sought are alloys based on common metals, such as Al, Cu, Fe, Co, and Ni [4–12].

A variety of Ni-based amorphous alloy systems have been developed so far [8–12]. Complex Ni–Nb–Cr–Mo–P–B alloys have been prepared in 1-mm-diameter amorphous rods [8]; amorphous rods of up to 2 mm in diameter have been fabricated in the Ni–Ti–Zr–(Si, Sn) system [9]; and in the complex, multi-component Ni–Nb–Ti–Zr–Co–Cu system amorphous rods of up to 3 mm in diameter have been found [10]. More recently, however, amorphous rectangular strips of up to 3 mm and 5 mm in thickness have been fabricated in the ternary Ni–Nb–Sn system and the quinary Ni–Cu–Ti–Zr–Al system, respectively [11,12]. The simple ternary Ni–Nb–Sn alloys exhibit exceptionally high Vickers hardness (1000–1280 kg/mm<sup>2</sup>), Young's modulus (180–200 GPa), and estimated strength (3–3.8 GPa).

\* Corresponding author.

E-mail address: [haein@sookmyung.ac.kr](mailto:haein@sookmyung.ac.kr) (H. Choi-Yim).

Additionally, these alloys show very high glass transition temperatures  $T_g$  of 881–895 K. In this paper, we report the results of systematic studies of structures, thermal, acoustic and mechanical properties, and small-angle neutron scattering (SANS) of the ternary Ni–Nb–Sn glass-forming alloys. A connection between the mechanical properties of these metallic glasses and their tendency to phase separation, as determined from the SANS experiments, is proposed and discussed.

## 2. Experimental methods

Ternary (and quaternary) alloy ingots were prepared by arc melting a mixture of ultrasonically-cleaned elements with a purity of  $\geq 99.7$  at.% in a Ti-gettered high-purity argon atmosphere. The alloyed ingots were then re-melted under high vacuum in a quartz tube using an induction-heating coil and then injected through a  $\sim 1$ – $1.5$  mm (inner diameter) nozzle into a copper mold using high-purity argon at a pressure of  $\sim 2$  bar. The copper molds have internal rod-shaped cavities of 30 mm in length and 2 mm in diameter, and strip-shaped cavities of 30 mm in length, 6 and 10 mm in width, and 0.5, 1, and 2 mm in thickness.

Transverse cross-sections of cast strips (cut along a plane normal to the length of the strip) were examined by X-ray diffraction (XRD), using a  $120^\circ$  position-sensitive detector (Inel) and a collimated Co  $K_\alpha$  X-ray source. The glass transition and crystallization behaviors of all samples were examined with a differential scanning calorimeter (Perkin–Elmer DSC 7). The DSC samples were also taken from cross-sectioned slices of the strips. Compression tests were performed on a universal testing machine (Instron 4200) at constant strain rates of between  $8 \times 10^{-5} \text{ s}^{-1}$  and  $3 \times 10^{-4} \text{ s}^{-1}$ . The strains were measured with strain gauges attached directly to the surface of the cylindrical samples, which had a diameter of 2 mm and an aspect ratio of 2–2.2. The ends of the cylinders were ground flat and perpendicular to the loading axis to an accuracy of less than 10  $\mu\text{m}$ . The compression test specimens were all examined with the X-ray diffractometer prior to the tests to ensure that they had fully amorphous structures. Two samples of each material were tested under identical conditions. The Vickers hardness of the samples was obtained using a Leitz micro-hardness tester. The Young's modulus, shear modulus and other acoustic properties were obtained by an ultrasonic-wave-propagation measurement. The Young's modulus data obtained from the two different approaches, i.e., the compression tests and the sound velocity measurements, were found to be in good agreement with each other.

The SANS measurements were performed at the Paul Scherrer Institute, Switzerland, on as-cast and annealed samples with dimensions 10 mm  $\times$  10 mm  $\times$  1 mm, using a wavelength of  $\lambda = 6 \text{ \AA}$  and sample–detector distances of 1.8, 6, and 20 m. Annealing was performed for several hours in a tube furnace under a vacuum of  $10^{-5}$  mbar.

## 3. Results and discussion

Fig. 1 shows XRD patterns of as-cast strips of compositions  $\text{Ni}_{60}\text{Nb}_{35}\text{Sn}_5$ ,  $\text{Ni}_{60}\text{Nb}_{33.1}\text{Sn}_{6.9}$ , and  $\text{Ni}_{60}\text{Nb}_{31}\text{Sn}_9$  with thicknesses of 1, 2, and 0.5 mm, respectively. The  $\text{Ni}_{60}\text{Nb}_{35}\text{Sn}_5$  and  $\text{Ni}_{60}\text{Nb}_{33.1}\text{Sn}_{6.9}$  samples exhibit broad diffraction maxima characteristic of metallic glasses with no evidence of any crystalline Bragg peaks. Based on this data, one may estimate that these two samples contain an at least  $\sim 98\%$  amorphous phase. The  $\text{Ni}_{60}\text{Nb}_{31}\text{Sn}_9$  strip shows XRD peaks from the crystalline  $\text{Ni}_2\text{NbSn}$  phase, superimposed on the broad diffuse scattering maxima from the amorphous phase. No noticeable traces of other phases were detectable within the sensitivity limit of XRD. We conclude that in these ternary alloys the maximum glass-forming ability is located at around  $6 \leq x \leq 7$ . With a higher Sn content (e.g.  $x = 9$ ), the  $\text{Ni}_2\text{NbSn}$  phase precipitates and coexists with the amorphous phase, thus forming a two-phase in situ composite.

The glass transition and the crystallization behavior of the as-cast strips, proved to be amorphous by XRD, were investigated using DSC at a heating rate of 0.33 K/s. Fig. 2 shows plots of  $T_g$  (onset temperature of glass transition) and  $T_{x1}$  (onset temperature of first crystallization event) as a function of the Sn concentration for glassy  $\text{Ni}_{60}\text{Nb}_{37}\text{Sn}_3$ ,  $\text{Ni}_{60}\text{Nb}_{35}\text{Sn}_5$ ,  $\text{Ni}_{60}\text{Nb}_{33.8}\text{Sn}_{6.2}$ , and  $\text{Ni}_{60}\text{Nb}_{33.1}\text{Sn}_{6.9}$  alloys.

The glass transition  $T_g$  decreases with an increasing Sn concentration, while the first crystallization temperature  $T_{x1}$  fluctuates when the Sn concentration is increased. Apparently, the maximal supercooled liquid region ( $\Delta T = T_{x1} - T_g$ ) is obtained for approximately 5 at.% Sn where  $\Delta \approx 58$  K. Compared with other Ni-based bulk metallic glasses, which generally have lower  $\Delta T$  values [8–12], the current Ni–Nb–Sn alloys are fairly resistant to crystallization upon heating. Thus these alloys are good candidates for consolidation processing, used for fabricating bulk metallic glasses of dimensions larger than their

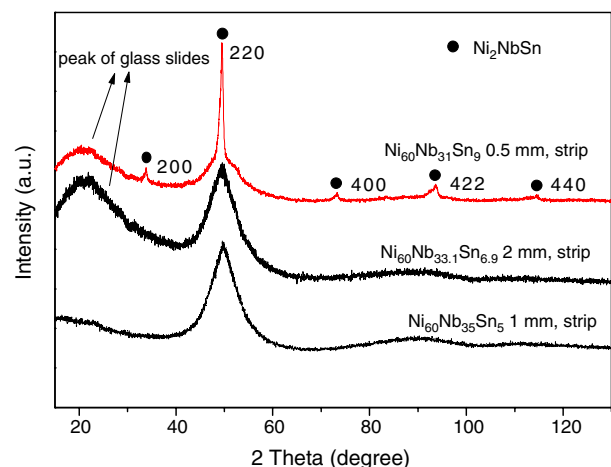


Fig. 1. XRD patterns of as-cast  $\text{Ni}_{60}\text{Nb}_{35}\text{Sn}_5$ ,  $\text{Ni}_{60}\text{Nb}_{33.1}\text{Sn}_{6.9}$ , and  $\text{Ni}_{60}\text{Nb}_{31}\text{Sn}_9$  strips, with thicknesses of 1, 2, and 0.5 mm, respectively.

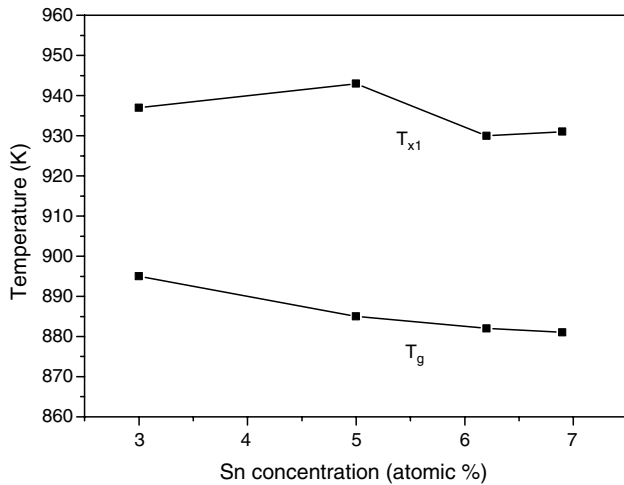


Fig. 2. Plots of  $T_g$  and  $T_{x1}$  (measured with DSC at a constant heating rate of 0.33 K/s) of glassy  $Ni_{60}Nb_{37}Sn_3$ ,  $Ni_{60}Nb_{35}Sn_5$ ,  $Ni_{60}Nb_{33.8}Sn_{6.2}$ , and  $Ni_{60}Nb_{33.1}Sn_{6.9}$  alloys as a function of Sn concentration.  $T_g$  is the onset temperature of the glass transition;  $T_{x1}$  is the onset temperature of the first crystallization event.

critical casting thickness (defined by the maximum thickness to which an amorphous alloy can be cast without crystallization).

Ultrasonic-wave-propagation measurements were performed on the glassy Ni–Nb–Sn alloys to reveal their acoustic and elastic properties. The propagation velocities of the longitudinal and transverse plane waves,  $C_l$  and  $C_s$ , can be directly obtained from these measurements, while the Young's modulus and the shear modulus can be calculated using the following relations (which are generally valid for isotropic materials such as metallic glasses):

- (1)  $\nu = (2 - x)/(2 - 2x)$ , where  $\nu$  is the Poisson ratio and  $x = (C_l/C_s)^2$ ,
- (2)  $G = \rho C_s^2$ , where  $G$  is the shear modulus and  $\rho$  is the density, obtained from a molar-volume-weighted average of the elemental densities, and
- (3)  $E = 2G(1 + \nu)$ , where  $E$  is the Young's modulus.

The acoustic and elastic data for the different glassy Ni–Nb–Sn alloys are presented in Table 1. It is noted that the moduli of the current alloys are among the highest reported to date for Ni-based BMGs [8–12], while the Poisson ratio is comparable to that of other Ni-based alloys (e.g.,  $\nu = 0.355$  for  $Ni_{40}Cu_5Ti_{16.5}Zr_{28.5}Al_{10}$  [12]).

In addition, compression tests were performed on the various  $Ni_{60}Nb_{40-x}Sn_x$  ( $x = 3, 5, 6.2, 6.9$ ) alloys. Fig. 3

Table 1  
Acoustic and elastic properties of various Ni–Nb–Sn alloys

| Alloy composition          | $C_l$ ( $10^3$ m/s) | $C_s$ ( $10^3$ m/s) | $\nu$ | $E$ (GPa) | $G$ (GPa) |
|----------------------------|---------------------|---------------------|-------|-----------|-----------|
| $Ni_{60}Nb_{37}Sn_3$       | 5.66                | 2.6                 | 0.37  | 199       | 58.6      |
| $Ni_{60}Nb_{35}Sn_5$       | 5.45                | 2.51                | 0.37  | 183       | 54.1      |
| $Ni_{60}Nb_{33.8}Sn_{6.2}$ | 5.49                | 2.53                | 0.36  | 184       | 54.8      |
| $Ni_{60}Nb_{33.1}Sn_{6.9}$ | 5.5                 | 2.54                | 0.36  | 185       | 55        |

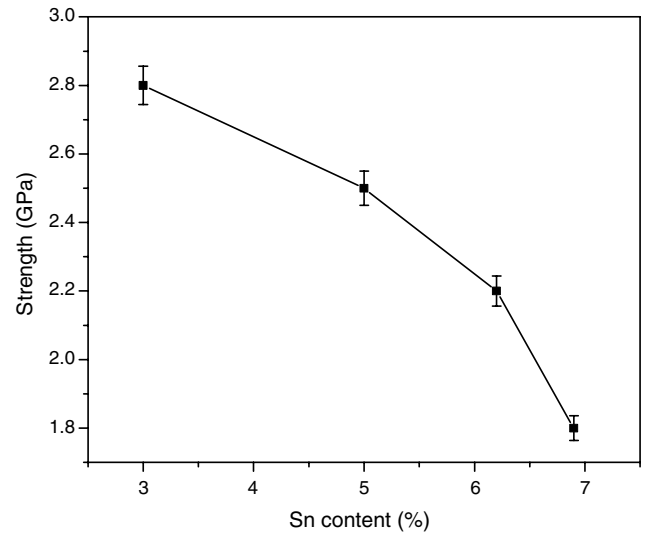


Fig. 3. Measured compressive strength of glassy  $Ni_{60}Nb_{37}Sn_3$ ,  $Ni_{60}Nb_{35}Sn_5$ ,  $Ni_{60}Nb_{33.8}Sn_{6.2}$ , and  $Ni_{60}Nb_{33.1}Sn_{6.9}$ . The strength of the  $Ni_{60}Nb_{40-x}Sn_x$  alloys decreases with an increasing Sn concentration.

shows the measured strength acquired in these tests as a function of the Sn concentration. Clearly, the measured strengths of the  $Ni_{60}Nb_{40-x}Sn_x$  alloys decrease rapidly with increasing Sn concentration, from 2.8 GPa at 3 at.% Sn to 1.8 GPa at 6.9 at.% Sn. Very brittle fracture occurred in the compressed alloys, which failed by the opening and propagation of cracks that had originated as small defects in the test specimens. Moreover, the compressive fracture did not take place along the maximum shear plane as in most metallic glasses.

From the Vicker's hardness ( $H_v$ ) test data [11] and the ultrasonic measurement results (Young's modulus,  $E$ , and shear modulus,  $G$ ), one would estimate the yield strength ( $\sigma_y$ ) of Ni–Nb–Sn alloys to be around 3.1 GPa to 3.8 GPa [11,13]. However, the compression tests that were performed showed that the Ni–Nb–Sn alloys fail prematurely, before the calculated yield strength is reached. Further, there is a strong compositional dependence of the apparent strength which cannot be explained by the slight variations in  $T_g$  or  $\nu$  with composition.

In previous work it was observed that phase separation occurs in many glass-forming alloy systems (e.g., Zr–Ti–Cu–Ni–Be(Al) [14,15] and Fe–Ni–P [16]) and may cause embrittlement in metallic glasses [17]. Finding out whether this is also true in the present Ni–Nb–Sn system may clarify the above mechanical test results. To investigate a possible phase separation in the current alloys, SANS measurements were carried out on as-prepared and annealed samples of varying compositions. Fig. 4, for example, shows the SANS intensity data of three  $Ni_{60}Nb_{33.8}Sn_{6.2}$  samples annealed at 853, 873 and 908 K, respectively, i.e. at various temperatures in the undercooled liquid state. An interference maximum is clearly seen for the two samples annealed for 12 h at 873 K and 6 h at 908 K, while SANS does not show scattering for the as-cast sample (not shown in Fig. 4). For the sample annealed for 12 h

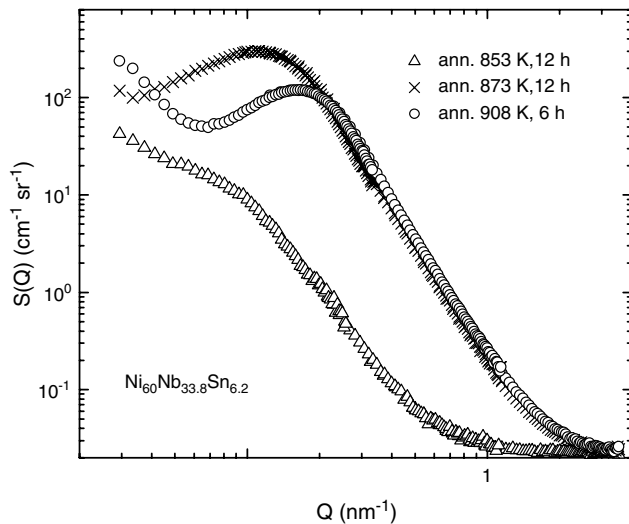


Fig. 4. SANS intensity data for three  $\text{Ni}_{60}\text{Nb}_{33.8}\text{Sn}_{6.2}$  samples annealed at various temperatures and times, as indicated in the figure ( $Q = 4\pi \sin \theta / \lambda$ , with  $\theta =$  half the scattering angle).

at 853 K, although no direct maximum appears, a rising hump on the intensity profile is noted as the precursor of a developing maximum.

Such interference maxima provide evidence of chemical inhomogeneities on the nanometer scale. Apparently these Ni–Nb–Sn alloys undergo phase separation and nanocrystallization upon annealing in the undercooled liquid state. Since the primary crystal phase in  $\text{Ni}_{60}\text{Nb}_{31}\text{Sn}_9$  is  $\text{Ni}_2\text{NbSn}$  (Fig. 1), we expect a substantial restructuring with regard to Ni/Nb and Sn to occur before primary crystallization sets in. Further evidence for this has also been obtained in a recently-performed independent anomalous X-ray scattering study [18]. Thus the discrepancy between the measured strength and the theoretically calculated strength, or in other words the premature fracture behaviors, of these refractory Ni-based BMGs may be interpreted as being a result of the alloys' tendency to phase separation. While further detailed investigations such as microscopy analyses on deformed or fractured samples are needed to find out how exactly the apparent phase separation may lead to the brittleness of the Ni–Nb–Sn glasses, a possible mechanism is as follows.

Upon cooling from their molten states the liquid alloys tend to phase separate, which produces local chemical inhomogeneities on very fine scales in the as-prepared state. At this stage these inhomogeneities are so fine that they are usually not detected by SANS; further, the time scale of the casting process is not large enough for crystallization to set in. These chemical inhomogeneities respond differently to an external stress in the different localized regions of the sample, since some of these regions may be more brittle than others. With increasing external stress, the weak phases then become the source of micro-cracks, which later result in the brittle failure of the samples. In addition, as can be deduced from Fig. 3, the alloys with higher Sn concentrations (e.g.,  $x = 6.9$ ) show a larger discrepancy

between their measured and calculated strengths than those with lower Sn content (e.g.,  $x = 3$ ), which may be explained by the alloys' different tendencies to phase separation.

#### 4. Conclusions

Bulk amorphous structures were formed by  $\text{Ni}_{60}\text{Nb}_{40-x}\text{Sn}_x$  ( $3 \leq x < 9$ ) alloys when cast in a metal mold. At high Sn concentrations (e.g.,  $x = 9$ ) a two-phase composite structure is formed with the  $\text{Ni}_2\text{NbSn}$  phase dispersed in the amorphous matrix. The ternary Ni-based BMGs exhibit high thermal stabilities with large glass transition temperatures ( $881 \text{ K} < T_g < 895 \text{ K}$ ) and wide undercooled liquid regions ( $40 \text{ K} < \Delta T < 60 \text{ K}$ ). The acoustic, elastic and mechanical properties of these amorphous alloys were measured. Compared with other reported Ni-based BMGs, the current alloys have very high elastic moduli and intermediate Poisson ratios. The apparent strength measured through compression tests is always lower than the theoretical strength estimated from the hardness and moduli and the degree of this discrepancy between the two strengths depends strongly on the Sn concentration. SANS suggests that these alloys tend to phase separate in the undercooled liquid state. Local chemical inhomogeneities arising from this tendency to phase separation are a possible reason for the embrittlement of these alloys and may also account for the strong compositional dependence of the measured strength.

#### Acknowledgements

The authors would like to acknowledge Greg Welsh and Gang Duan for their help with the mechanical tests.

#### References

- [1] Inoue A, Zhang T, Masumoto T. *Mater Trans JIM* 1990;31:425.
- [2] Zhang T, Inoue A, Masumoto T. *Mater Trans JIM* 1991;32:1005.
- [3] Peker A, Johnson WL. *Appl Phys Lett* 1993;63:2342.
- [4] Xu DH, Duan G, Johnson WL. *Phys Rev Lett* 2004;92:245504.
- [5] Xu DH, Lohwongwatana B, Duan G, Johnson WL, Garland C. *Acta Mater* 2004;52:2621.
- [6] Lu ZP, Liu CT, Thompson JR, Porter WD. *Phys Rev Lett* 2004;92:245503.
- [7] Ponnambalam V, Poon SJ, Shiflet GJ. *J Mater Res* 2004;19:1320.
- [8] Wang XM, Yoshii I, Inoue A, Kim YH, Kim IB. *Mater Trans, JIM* 1999;40:1130.
- [9] Yi S, Lee JK, Kim WT, Kim DH. *J Non-Cryst Solids* 2001;291:132.
- [10] Zhang T, Inoue A. *Mater Trans, JIM* 2002;43:708.
- [11] Choi-Yim H, Xu DH, Johnson WL. *Appl Phys Lett* 2003;82:1030.
- [12] Xu DH, Duan G, Johnson WL, Garland C. *Acta Mater* 2004;52:3493.
- [13] Most of BMGs observe the approximate relations:  $\sigma_y \approx H_v/3$  and  $\sigma_y \approx E/50$ . The latter relation comes from the fact that most of BMGs have a yield strain  $\sim 2\%$ .
- [14] Löffler JF, Johnson WL. *Appl Phys Lett* 2000;76:3394.
- [15] Löffler JF, Bossuyt S, Glade SC, Johnson WL, Wagner W, Thiyagarajan P. *Appl Phys Lett* 2000;77:525.
- [16] Gerling R, Schimansky FP, Wagner R. *Nucl Sci Eng* 1992;110:374.
- [17] Gerling R, Schimansky FP, Wagner R. *Acta Metall* 1988;36:575.
- [18] Billelo JC et al. Unpublished results.